Int J Thermophys (2014) 35:2062–2070
DOI 10.1007/s10765-014-1735-9

Signal-to-Noise Analysis of the Improved Open Photoacoustic Helmholtz Cell

Antonina Geras

Received: 14 April 2014 / Accepted: 26 August 2014 / Published online: 29 October 2014

Abstract Open photoacoustic cells are often used in continuous-flow photoacoustic measurements. Such cells are sensitive to external noise penetration. The improved open photoacoustic Helmholtz cell has much better external noise attenuation than the previously known designs. This paper describes how mechanical dimensions of such a cell influence its signal-to-noise ratio. The analysis was performed by means of computer simulations based on the loss-improved transmission line model. This research showed that the mechanical parameters affect signal-to-noise noticeably and, if they are properly chosen and applied in the design of the improved open cell, the resulting signal-to-noise ratio may be improved by almost 60 dB in comparison to previous designs of open photoacoustic Helmholtz cells.

Keywords External noise attenuation · Helmholtz resonator · Open photoacoustic cell · Parametric analysis · Photoacoustic cell improvement · Signal-to-noise ratio

1 Introduction

In photoacoustic measurements of fluids, open photoacoustic cells are usually much more convenient than closed ones. This is due to the fact that they allow for straightforward gas or liquid exchange between the cell and the environment, what simplifies measurement instrumentation and processes [1–3]. The consequence of opening the cell to the environment is that along with the gas, external acoustic noise penetrates the cell's interior. This is not crucial in the case of smoke detectors, when the amount of absorbent is significant, and the induced photoacoustic signal is strong [3]. The

A. Geras (✉)
Institute of Electronic Systems, Warsaw University of Technology,
Nowowiejska 15/19, 00-665 Warsaw, Poland
e-mail: antonina@geras.pl

problem arises when there is a demand for sensing low concentrations of a substance. In such a case, the photoacoustic signal may even be a few orders of magnitude weaker than the external noise, so its occurrence can seriously affect the measurements [4–6]. Definitely, the external acoustic noise should be attenuated or filtered out. One of the commonly used techniques is to incorporate cells of big volumes, acting as acoustic buffers. This paper presents parametric analysis of signal-to-noise ratio of an improved open photoacoustic Helmholtz cell, previously presented by Starecki and Geras [7].

2 Open Photoacoustic Helmholtz Cell

As was previously stated, the photoacoustic signal can be very low and would be difficult to detect even by an extremely sensitive microphone [8,9]. To amplify the signal, the acoustic resonance of the chamber may be used. There are a number of open windowless cells reported in the literature, and in most cases, signal amplification is based on the standing wave resonances [1–3,10–14]. Such cells are usually of relatively large volumes, so their applications are strongly limited. Another kind of a photoacoustic resonant cell is the Helmholtz resonator, which usually has a volume of just a few cubic centimeters. Open cells of this kind were proposed by Diószhegy et al. [6] and by Starecki [15], but because of their sensitivity to the external acoustic noise, they are of no practical use in standard environments. To overcome this limitation, a new design of an open photoacoustic cell was proposed by Starecki and Geras [7], as shown in Fig. 1.

The presented cell is an improved version of the open windowless photoacoustic Helmholtz cell [15]. Its main part is the Helmholtz resonator to which the two acoustic buffers are attached via coaxial ducts of relatively small diameter (denoted as 'internal ducts'). The cell is opened to the ambient by means of the so-called 'external ducts.' These ducts are located aside the optical path of the light beam. The cell is equipped with windows, which will introduce a parasitic background signal [16]. As the buffers are of a relatively large volume, this signal will be strongly attenuated.

The Helmholtz resonator consists of a sample cavity and a microphone cavity, connected by a thin duct. In such cells, despite their small size, the resonance frequency is quite low. It is advantageous, because the amplitude of photoacoustic signal is inversely proportional to the cell volume and to the light beam modulation frequency:

$$A \propto \frac{\alpha P}{f V}, \tag{1}$$

where α is the light absorption coefficient, P is the light power, f is the light intensity modulation frequency, and V is the volume of the cell [17,18].

To amplify the photoacoustic signal, the modulation frequency of the light beam should be adjusted to an acoustic resonance of the cell [4,14,15,19]. Thus, if the resonance frequency is low, the modulation frequency would also be low. Furthermore, due to separation of the cavities by a narrow duct, Helmholtz cells allow for good isolation of the microphone from the sample and the light beam. In single-cavity cells, where such isolation does not exist, the incident light beam can result in an increase of the background noise [15,18,20,21]. The mechanism of photoacoustic

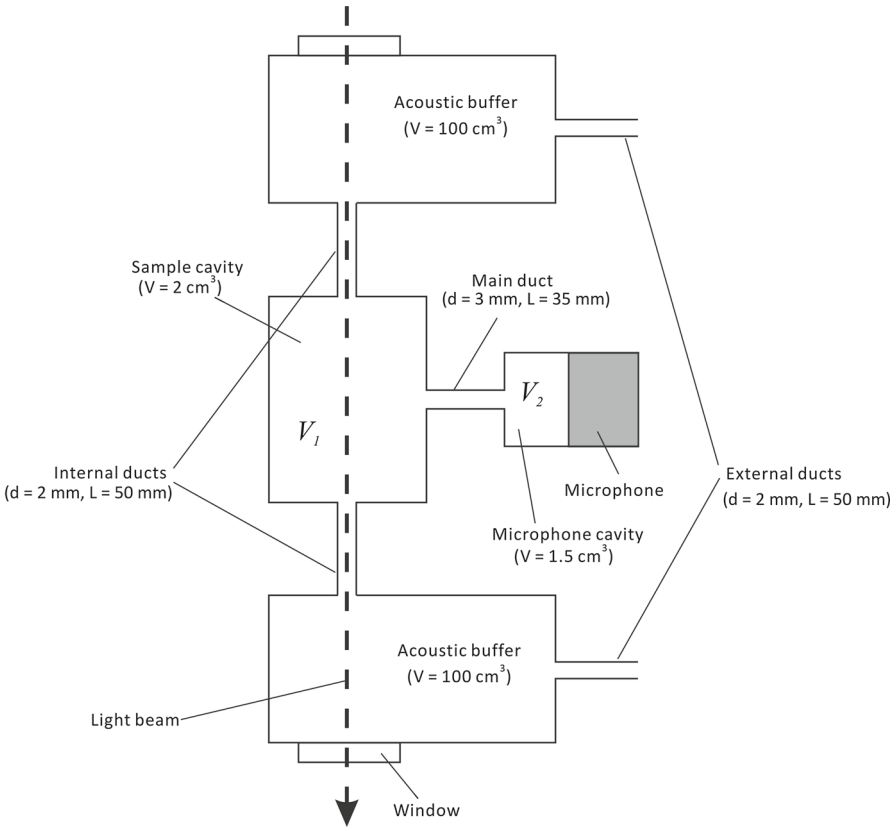

Fig. 1 Improved open photoacoustic Helmholtz cell with dimensions as in the reference cell [7]

signal triggering in the Helmholtz resonator is quite different from that in the other kinds of resonance cells (such as those with the standing wave resonance) [14,22]; the sample is illuminated by the light of the frequency in the sample's absorption spectrum. As a result of light absorption, the temperature of the gas inside the sample cavity increases, and the gas expands and moves to the microphone cavity. When the absorption is halted (by turning off the light source), the gas flows in the opposite direction. In such a way, the modulated light beam causes a periodic flow of the gas between the cavities, thus generating thermal and sound waves [1,6,19,23]. The resonance frequency of this process is given by the equation,

$$f_{\mathrm{res}} = \frac{vd}{4\pi}\sqrt{\frac{\pi}{l}\frac{V_1 + V_2}{V_1 V_2}}, \tag{2}$$

where V_1 and V_2 are the sample and microphone cavity volumes, l is the length of the duct, d is the diameter of the duct, and v is the sound speed in the gas filling the cell. This frequency can be adjusted in a very simple way, i.e., by selecting appropriate volumes of the cavities and dimensions of the main duct [15,24].

In the proposed cell (Fig. 1), two symmetrical acoustic buffers are connected to the resonator by thin ducts. The ducts can be treated as acoustic transmission lines if the length of the internal and external ducts is equal to a quarter of the acoustic wave corresponding to the frequency of the resonance. The input impedance of such a line is inversely proportional to the load at its end, so placing a buffer of a big volume (thus, small impedance) would make this line act as a high acoustic impedance for the external signals [4], according to the formula,

$$Z_{\mathrm{i}} = \frac{Z_{\omega}^2}{Z_{\mathrm{l}}}, \tag{3}$$

where Z_{i}, Z_{l}, and Z_{ω} are the input, load, and characteristic impedance of the line, respectively [5]. It means that the buffers, connected via ducts of a properly chosen length, should help to prevent external noise infiltration. Furthermore, it was observed that dimensions of the ducts and buffers have a noticeable impact on the external noise attenuation and that their proper selection can significantly improve cell properties [1,25]. An important measure, which indicates a level of sensitivity that can be obtained with a given open cell design, is its ability to attenuate external acoustic noise, which can be expressed by the signal-to-noise ratio. To find a dependency between the dimensions and signal-to-noise ratio, parametric analysis was performed.

3 Modeling Method

To calculate the signal-to-noise ratio, it was necessary to determine the frequency response and values of the external noise attenuation for the given frequency range. These graphs were obtained by means of loss-improved electroacoustic modeling. The method has already been tested and proven to give accurate results [17,20,25,27]. Modeling allows examination of some of the cell properties before its manufacture. In the case of the discussed cell, some of the ducts may have very small diameters and be relatively long. As per the above, it was essential to use computer modeling in order to find optimal values of dimensions that would be used for future cell manufacture.

The principle of the acousto-electric analogies is to create a model of a cell in which each of its acoustic parts is replaced by its electric counterpart, i.e., the cavity corresponds to capacitance, and the ducts are replaced by transmission lines converted into corresponding T-section impedances [20,26]. In the literature, different definitions for calculation of values of the electric counterparts can be found [20,21,24,28,29]; however, the best results are obtained when the loss-improved method is applied [17]. The model used in the analysis of the improved cell was described in considerable detail in previous papers [7,26].

4 Modeling Results

As previously stated, the aim of the modeling was to discover how each of the cell dimensions influences the cell's behavior. First, a reference cell was examined. The dimensions of this cell remained unchanged and were the following: sample and

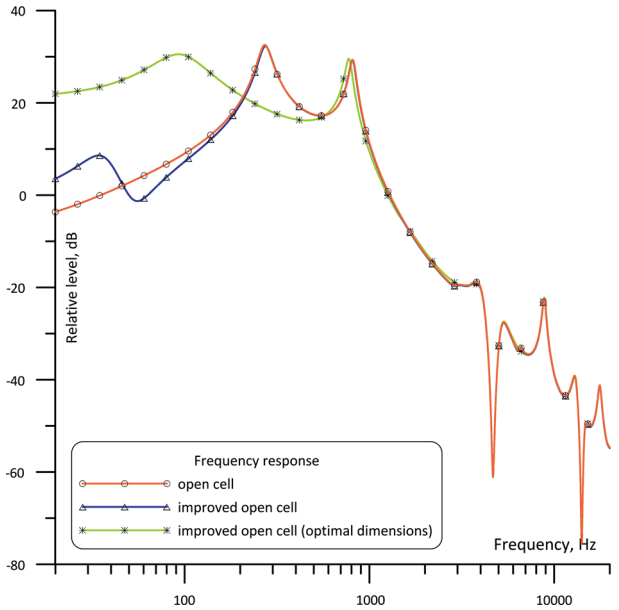

Fig. 2 Frequency responses of the open cell, the improved cell (with buffers), and the improved cell with optimal dimensions

microphone cavities of 2 cm^3 and 1.5 cm^3, respectively, buffers had volumes of 100 cm^3, the main duct length was equal to 35 mm, the diameter was 3 mm, and internal and external ducts were 50 mm long and 2 mm in diameter. In the case of such dimensions, the resonance should occur at about 800 Hz (according to Eq. 1), which was confirmed by the frequency response presented in Fig. 2 which shows frequency responses of two types of open Helmholtz cells: a basic open cell and the improved cell (with buffers). It can be concluded that in the region of the resonance frequency, parts additional to the resonator (i.e., ducts and buffers) do not influence the frequency response of the cell. These considerations were extensively presented in previous papers [7,26].

The signal-to-noise ratio of the investigated cell is shown in Fig. 3. From that graph, one can conclude that in comparison to the basic open cell, the signal-to-noise ratio of the improved cell is greater by almost 50 dB. It should be stated that experimental values of the signal-to-noise ratio in the high frequency region (above f_0) will be slightly different from those obtained by means of simulations. In practice, the signal-to-noise ratio will be affected by the level of noise from the other sources. Taking into consideration that the amplitude of the signal above the resonance frequency f_0 decreases rapidly with the frequency, the practically obtained signal-to-noise ratio would be lower than the theoretical one.

To determine the influence of each of the dimensions, at one simulation, only one dimension was changed. The length of the ducts was changed in the range from 25 mm to 150 mm with a step of 25 mm, and the diameters were changed from 1 mm to 3 mm with a step of 0.5 mm. In case of the internal, as well as the external duct lengths, the best

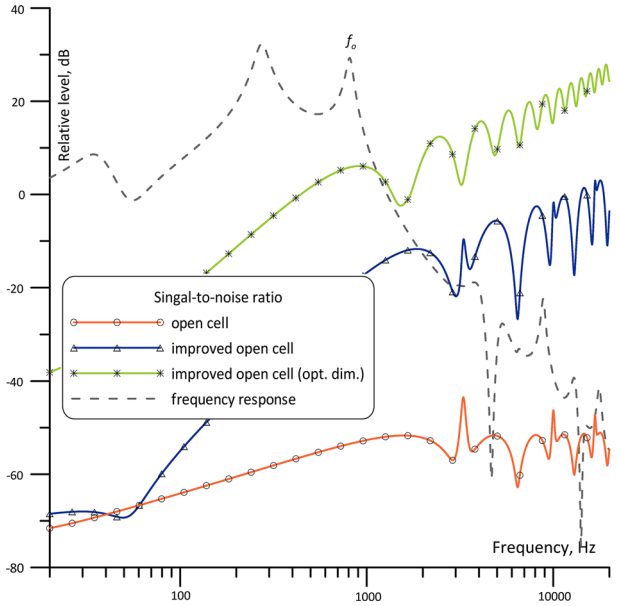

Fig. 3 Comparison of signal-to-noise ratio of the reference open cell, the reference improved open cell, and the improved cell with optimal dimensions

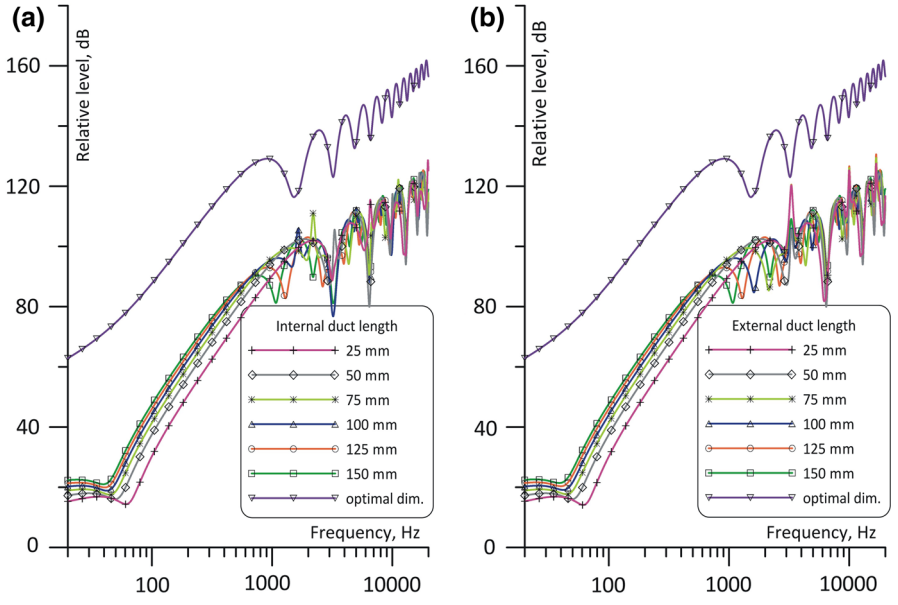

Fig. 4 Signal-to-noise ratio of the improved cell with different (a) internal and (b) external duct lengths

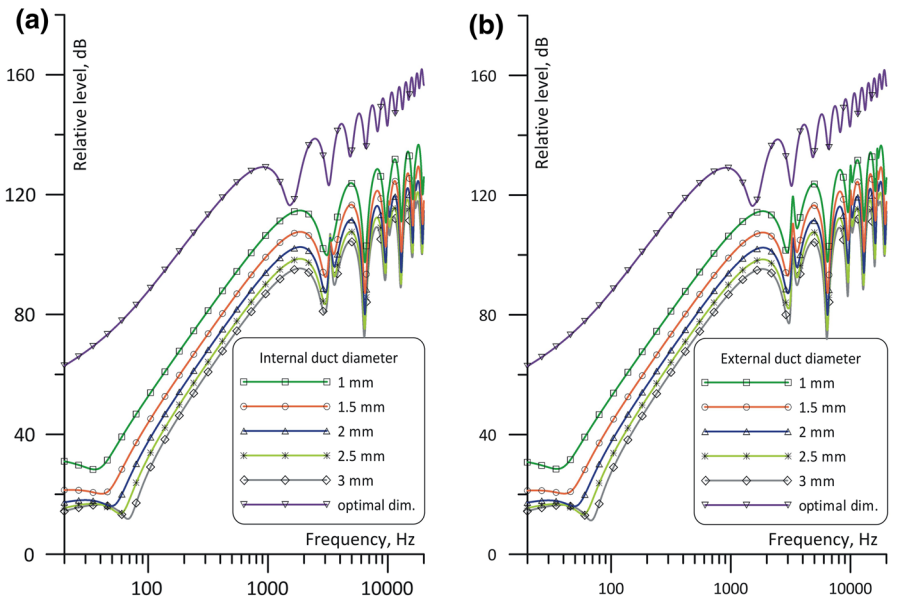

Fig. 5 Signal-to-noise ratio of the improved cell with different (a) internal and (b) external duct diameters

signal-to-noise ratio at the resonance frequency was obtained for a value of 100 mm, which is not the smallest nor the greatest among those examined (Fig. 4). The result is not surprising, as this value is close to a quarter of the wavelength of the induced acoustic wave. In the case of the ducts' diameter, the smallest one results in the best external noise attenuation, giving the best signal-to-noise ratio (Fig. 5). Manufacture of such a duct, especially at a length of 100 mm (which, as was already stated, should lead to the best signal-to-noise ratio), would be very difficult. What is more, internal ducts form a channel through which the light beam is passed. The other potential inconvenience is that the smaller the duct diameter, the slower is the gas exchange. When a fast response of the sensor is required, low volumetric flow rates may be not acceptable [4]. Thus, it is worth noting that in the case of the 2 mm diameter duct, the signal-to-noise ratio is worse only by about 20 dB in comparison to the one obtained with the diameter of 1 mm. When considering the buffers volumes, it is quite obvious that a greater volume results in a higher signal-to-noise ratio (Fig. 6). Theoretically, there is no limit for increasing the buffer volume, but in practical applications, that would significantly enlarge the cell and slow down the gas exchange [4].

As a final step, modeling of a cell with dimensions that resulted in the best signal-to-noise ratio at each preceding simulation was performed. These graphs are denoted as 'optimal dimensions' in Figs. 2, 3, 4, 5, and 6. It is clearly visible that a cell of such dimensions (ducts 100 mm long and 1 mm in diameter, buffers of 250 cm^3) is characterized by a signal-to-noise ratio much better than in the case when only one of the dimensions is optimal. When comparing a cell with 'optimal' dimensions to an open cell presented in [7] and [27], the signal-to-noise ratio is greater by almost 60 dB (Fig. 3). Furthermore, not all possible combinations of dimensions were examined, so there may still be room for future improvement.

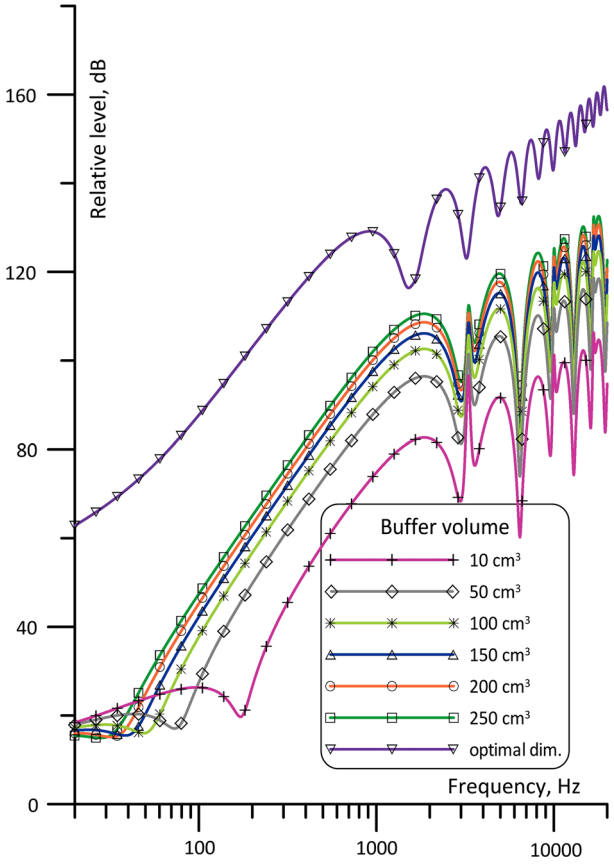

Fig. 6 Signal-to-noise ratio of the improved cell with different volumes of the buffers

5 Conclusions

The presented analysis shows that the signal-to-noise ratio of the improved open Helmholtz photoacoustic cell may be considerably increased as a result of a deliberate choice of the cell's components. The best results are obtained in the case when a combination of optimal parameters is applied. Most attention should be paid to the length of the ducts since selection of this parameter is not straightforward, as the optimal value is not an extreme one. Decrementing the ducts diameters results in an improvement of the signal-to-noise ratio. In the case of the buffers, the best noise rejection is obtained for the greatest volume, so their size is limited by practical requirements such as the total cell size and the expected flow rate.

References

1. A. Miklós, A. Lörincz, Appl. Phys. B **48**, 213 (1989)
2. D.H. McQueen, J. Phys. E Sci. Instrum. **16**, 738 (1983)
3. A. Keller, M. Rüegg, M. Forster, M. Loepfe, R. Pleisch, P. Nebiker, H. Burtscher, Sens. Actuators B **104**, 1 (2005)
4. Z. Bozóki, A. Szabó, Á. Mohácsi, G. Szabó, Sens. Actuators B **147**, 206 (2010)
5. T. Starecki, Acta Phys. Pol. A **114**, 199 (2008)
6. T. Diószeghy, A. Miklós, A. Kelemen, A. Lörincz, J. Appl. Phys. **58**, 2105 (1985)
7. T. Starecki, A. Geras, Int. J. Thermophys. (2013). doi:10.1007/s10765-013-1479-y
8. I.G. Calasso, M.W. Sigrist, Rev. Sci. Instrum. **70**, 4569 (1999)
9. M.H. de Paula, C.A. Vinha, R.G. Badini, Rev. Sci. Instrum. **63**, 3487 (1992)
10. Z. Bozóki, J. Sneider, G. Szabó, A. Miklós, M. Serényi, G. Nagy, M. Fehér, Appl. Phys. B **63**, 399 (1996)
11. A. Boschetti, D. Bassi, E. Iacob, S. Iannotta, L. Ricci, M. Scotoni, Appl. Phys. B **74**, 273 (2002)
12. S. Schäfer, A. Miklós, P. Hess, Appl. Opt. **36**, 3202 (1997)
13. M.D. da Silva, I.N. Bandeira, L.C.M. Miranda, J. Phys. E Sci. Instrum. **20**, 1476 (1987)
14. Ch. Brand, A. Winkler, P. Hess, Z. Bozóki, J. Sneider, Appl. Opt. **34**, 3257 (1995)
15. T. Starecki, Acta Phys. Pol. A **114**, 211 (2008)
16. A.V. Gorelik, V.S. Starovoitov, Opt. Spectros. **107**, 830 (2009)
17. T. Starecki, J. Acoust. Soc. Am. **122**, 2118 (2007)
18. V. Zeninari, V.A. Kapitanov, D. Curtois, Y. Ponomarev, Infrared Phys. Technol. **40**, 1 (1999)
19. B. Baumann, B. Kost, M. Wolff, H. Groninga, T. Blöß, S. Knickrehm, *Numerical Shape Optimization of Photoacoustic Sample Cells: First Results*, Proc. of the COMSOL Users Conference (Grenoble, France, 2007).
20. O. Nordhaus, J. Pelzl, Appl. Phys. **25**, 221 (1981)
21. R. Kästle, M.W. Sigrist, Appl. Phys. B **63**, 389 (1996)
22. C.F. Dewey, R.D. Kamm, C.E. Hackett, Appl. Phys. Lett. **23**, 11 (1973)
23. P. Hess, *Springer Series in Optical Sciences, Photoacoustic and Phenomena ll*, vol. 62 (Springer, Berlin, 1990), pp. 336–343
24. A. Rosencwaig, A. Gersho, J. Appl. Phys. **47**, 64 (1976)
25. T. Starecki, K. Opalska, A. Burd, S. Misiaszek, M. Ramotowski, Proc. SPIE **5948**, 702 (2005)
26. A. Geras, T. Starecki, Int. J. Thermophys. doi:10.1007/s10765-013-1497-9
27. T. Starecki, Proc. SPIE **6159**, 698 (2006)
28. M. Suchenek, Proc. SPIE **6937**, 693711 (2007)
29. M. Mattiello, M. Niklès, S. Schilt, L. Thévenaz, A. Salhi, D. Bart, Y. Rouillard, R. Werner, J. Koeth, Spectrochem. Acta A **63**, 952 (2006)